

## Flood Inundation Mapping for Porsuk Stream, Eskişehir, Turkey

M. Murat Kale<sup>1</sup>, Murat Ataol<sup>2</sup>

### Abstract

Flood is one of the most widespread and catastrophic natural hazards for settlements in different parts of the world. Eskişehir has faced numerous floods at varying scales, especially in the last century. Porsuk Stream moves in an artificial channel through the Eskişehir city center. The bed of Porsuk Stream is expanded and cascaded at the entrance to the city center, and the stream has been turned into one of the attractions of the city by increasing its water level with nine regulators. Expanding the river bed is a frequently used method to reduce flood risk. However, in Eskişehir, the fact that the river bed is kept largely filled with water is a major source of risk in case of flooding. The study is based on a scenario in which flooding occurs due to the failure of regulator covers to open. In the study field, the sensitivity of the numerical field model that was created along the stream bed was further improved by measuring lengths and depths throughout the channel. Within the framework of the scenario, the water levels that can change with flood discharges were determined, and inundation areas were calculated. The results revealed that, according to the flood discharges in Porsuk Stream with probabilities of occurrence in every 50, 100, and 200 years, areas of 3.20 km<sup>2</sup>, 4.03 km<sup>2</sup>, and 4.48 km<sup>2</sup> would be flooded, respectively. The maximum discharge with a return period of 200 years ( $Q_{200}$ ) is 194.46 m<sup>3</sup>/s, which, if realized, would result in inundation of 1.58 km<sup>2</sup> of residential areas and 0.55 km<sup>2</sup> of agricultural land. Of the total flood area, 35% will be residential areas, 33% will be airports, 12% will be agricultural lands, 9% will be green areas, 7% will be industrial areas and 3% will be sports facilities.

**Keywords:** Flood Inundation Mapping, Porsuk Stream, HEC-RAS, Eskişehir

### 1. INTRODUCTION

Flooding is a natural process involving the overflowing of land that is not submerged by a body of water (Ward, 1978; Baker, 2013; Berghuijs et al. 2019). Natural disaster statistics show that the number of floods has tended to increase more in recent years when compared to other natural disasters (CRED, 2003; Dutta and Herath, 2004; URL 1; Dottori et al. 2018). According to the trend analyses for natural disasters, the frequency of floods has also increased in recent years (Berz, 2001; Kleinen and Petschel-Held, 2007; Shi et al. 2020; Pinos and Quesada-Román, 2021).

Natural and anthropogenic factors have important roles in flood causation (Simonovic, 2012). Anthropogenic factors may directly stem from human-built structures (dams, regulators, channels, water reservoirs etc.) and erroneous urbanization policies, or they may be an indirect product of the pressure on the climate system. During the period from the Industrial Revolution to today, Earth's climate system has been put under great pressure. Due to that pressure, the number and frequency of flood disasters have increased in different geographies (McCabe et al.,

<sup>1</sup> Assoc.Prof., Department of Geography, Çankırı Karatekin University, Çankırı  
e-mail: mmuratkale@gmail.com ORCID No: 0000-0001-6975-7069

<sup>2</sup> Assoc.Prof., Department of Geography, Çankırı Karatekin University, Çankırı  
Corresponding author e-mail: murat.ataol@gmail.com ORCID No: 0000-0002-3213-0972

1997; Milly et al., 2002; Hirabayashi et al., 2013; Özdemir and Leloğlu, 2014; Amellah et al. 2020; Dahri and Abida, 2020; Kaya Melisa et al., 2020). Global climate change also causes an increase in seasonal anomalies (McCabe et al., 1997; Korkmaz, 2022a).

Cities are expanding, with or without planning, on a global scale due to the increasing human population. With that expansion come changes in the land use in cities. Today, city centers are faced with greater risk of flood due to changing land use and climate (Ashley et al., 2005; Chang and Franczyk, 2008; Huong and Pathirana, 2013; Li et al., 2013; Erkal and Barış, 2013). The abundance of impervious surfaces in urban areas also increases the risk of flooding. A large part of the precipitation begins to flow on impervious surfaces (Scalenghe and Marsan, 2009; Strohbach et al., 2019). The increase in impervious areas in cities and the conversion of a greater proportion of precipitation to runoff, increase the frequency of flooding (Cutter et al., 2018). One of the key factors in assessing flood risk is to determine the recurrence interval of floods, or the frequency at which floods of a certain magnitude are expected to occur (Korkmaz, 2022b).

Between 1998 and 2017, two billion people around the world were affected by floods, and floods caused economic losses of over 656 billion dollars (URL 1). Of the natural disasters occurring during that period, 43.4% were floods (URL 1). The number of people who lost their lives due to floods was over 8000 in 2010 alone (URL 2). Within that framework, determining the frequencies of floods and their effects and appropriate responses by decision makers to those results have vital roles in the management of disaster scenarios. For the determination of high-risk areas based on the increased global flood rate, the importance of flood inundation mapping and land planning according to that mapping has gradually increased (Chen et al., 2009; Masood and Takeuchi, 2012; Alfieri et al., 2014; Bharath and Elshorbagy, 2018). HEC-RAS (Hydrologic Engineering Center's River Analysis System) software is also frequently used in flood analysis (Tate and Maidment, 1999; Yang et al., 2006; Quiroga et al., 2016; Costabile et al., 2020; Namara et al., 2022).

In Turkey, similar to the worldwide trend, flooding is the second most devastating natural disaster type, after earthquakes that cause loss of lives and economic damage. Between 1955 and 2012, 1480 people have died, and billions of dollars have been lost due to floods in Turkey (OSİB, 2015).

The study area, Eskişehir, is in the western region of Central Anatolia. It is among the important industrial and residential centers of Turkey. Eskişehir has faced numerous floods at varying scales, especially in the last century (URL 3). In the twentieth Century, two large flood disasters occurred in the Eskişehir city center due to Porsuk Stream. The first of those floods occurred in 1909 (Koylu, 2008), and the more recent flood occurred in March of 1950 (Şimşek, 2014). Archival records show that the flood in 1950 destroyed 3000 housing units (TBMM, 1950) and caused a severe housing problem when thousands of people became homeless.

Eskişehir city center, which is among the most important cities in Anatolia Peninsula, is developing in the floodplain of the Porsuk Stream and its surroundings. In general, flood events in Eskişehir city center may occur due to scenarios originating from excessive precipitation, dam failure, or regulator failure. In this context, numerous flood studies have been carried out for Eskişehir. Haltas et al. (2016) focused on a dam failure for various dam breaching scenarios and utilized the numerical modeling of the propagation of flood waves downstream of the dam. Bayazit et al. (2019) aimed to develop the flood risk analysis of the Porsuk River by utilizing the methods of Remote Sensing (RS) and Geographical Information Systems (GIS). In addition, a regulator-based flood study has not been investigated for Eskişehir city center.

In the study, a flood scenario was created for Porsuk Stream, which passes through the Eskişehir city center and moves in an artificial channel. Models were formulated on the basis of the scenario, and answers were sought as to how the flood would be distributed in the city center and which

areas would be flooded. Thus, in the present study the high-risk regions according to the disaster scenario were determined.

The overall goal of the present study is to create the flood inundation maps of Eskişehir city center based on the flood scenario in which the regulator covers fail to open. Also, this paper contributes the scientific knowledge to evaluating the flood outputs obtained from previous studies (excessive precipitation and dam failure), and the regulator-based flood outputs of this study will help the decision-makers to reach more accurate results.

### 1.1. Study Area

Porsuk Stream is one of the main tributaries of the Sakarya River and has a drainage area of  $\sim 10147 \text{ km}^2$ . It drains 6% of the Sakarya Basin, and its main tributary is  $\sim 460 \text{ km}$  long. The foothills of Murat Mountain in Kütahya are the source of the river. The drainage area of Porsuk Stream includes the city centers of Eskişehir and Kütahya. The study deals with the western part of the Porsuk Basin, extending to the stream's exit at the Eskişehir city center. The Upper Porsuk Basin has a drainage area of  $\sim 6442 \text{ km}^2$  and is situated between  $38^\circ 44'$  and  $39^\circ 55' \text{ N}$  latitude and  $29^\circ 38'$  and  $30^\circ 34' \text{ E}$  longitude. Precipitation in the basin is transported by Porsuk Stream to the Sakarya River through the artificial waterways passing through the Eskişehir city center (Figure 1).

In the study region, the most important tributaries of Porsuk Stream are Çat, Sarısu, Sabuncupınarı and Ilıca streams (Figure 1). Sarısu Stream drains the north of the basin, while Sabuncupınarı and Ilıca streams drain the northeast of the basin. Çat Stream drains the southeast of the basin.

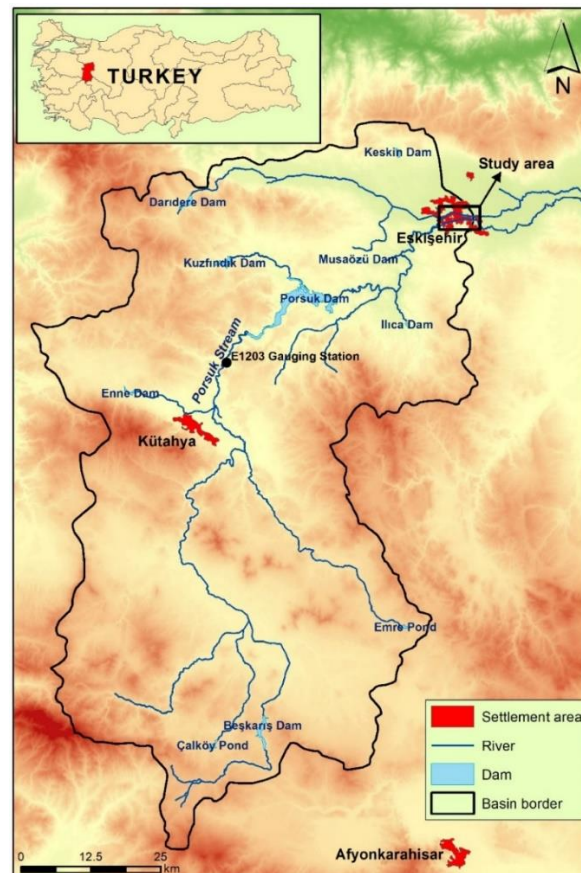


Figure 1. Western part of the Porsuk Basin (Upper Porsuk Basin)

Characteristics of two different climates are observed in the basin. In the southern part of the basin, a Mediterranean transition climate is observed, while continental climate is observed in the areas to the north of Kütahya (Sarış et al., 2010). Tables 1 and 2 show the long-term temperature and precipitation parameters of the meteorological observation stations for Eskişehir and Kütahya, which are located upstream of study field.

Table 1. Long-term mean monthly temperature (°C)

Station	Month											
	JAN	FEB	MAR	APR	MAY	JUN	JUL	AUG	SEP	OCT	NOV	DEC
Kütahya	0.3	1.6	5.0	10.0	14.4	18.3	20.7	20.2	16.4	11.6	6.2	1.9
Eskişehir	-0.5	1.1	5.0	10.0	14.9	19.0	21.9	21.4	16.9	11.8	5.8	1.1

Source: Eskişehir and Kütahya Meteorological Stations

Table 2. Long-term monthly precipitation (mm)

Station	Month											
	JAN	FEB	MAR	APR	MAY	JUN	JUL	AUG	SEP	OCT	NOV	DEC
Kütahya	65.3	55.3	52.8	56.7	50.6	31.4	19.4	16.9	22.0	44.0	55.4	78.3
Eskişehir	38.8	28.8	33.3	43.7	45.7	28.6	14.5	10.0	14.3	30.8	32.9	42.7

Source: Eskişehir and Kütahya Meteorological Stations

According to the long-term monthly temperature data, the lowest temperature values are observed in December, January, and February. The highest and lowest mean monthly temperatures were recorded in July (21.9 °C) and January (-0.5 °C) at the Eskişehir meteorological observation station, respectively. According to the long-term precipitation data (1975-2008), July, August, and September are the driest months. A decreasing trend in precipitation prevails were determined in autumn (Çiçek and Duman, 2015). Above-average precipitation was recorded in December and January at the Kütahya meteorological observation station and in April, May, and December at the Eskişehir meteorological observation station.

Along the Kütahya–Eskişehir axis, the area drained by Porsuk Stream’s flow is characterized by high temperature and low precipitation values (Figure 2). The region near Kütahya, with the highest precipitation amount, also has the lowest mean temperature value. Considering the long-term data, the west axis of the basin receives more precipitation than its northeast axis (Figure 2).

Porsuk Stream moves in an artificial channel through the Eskişehir city center. The bed of Porsuk Stream is expanded and cascaded at the entrance to the city center, and the stream has been turned into one of the attractions of the city by increasing its water level with nine regulators (Figure 3). Water of about four meters depth is held in a nearly thirty-meter-wide channel by the regulators. The portion of the channel above the water level is nearly two meters high. That height forms the channel level that would be subject to sudden discharges if regulator covers do not open rapidly.

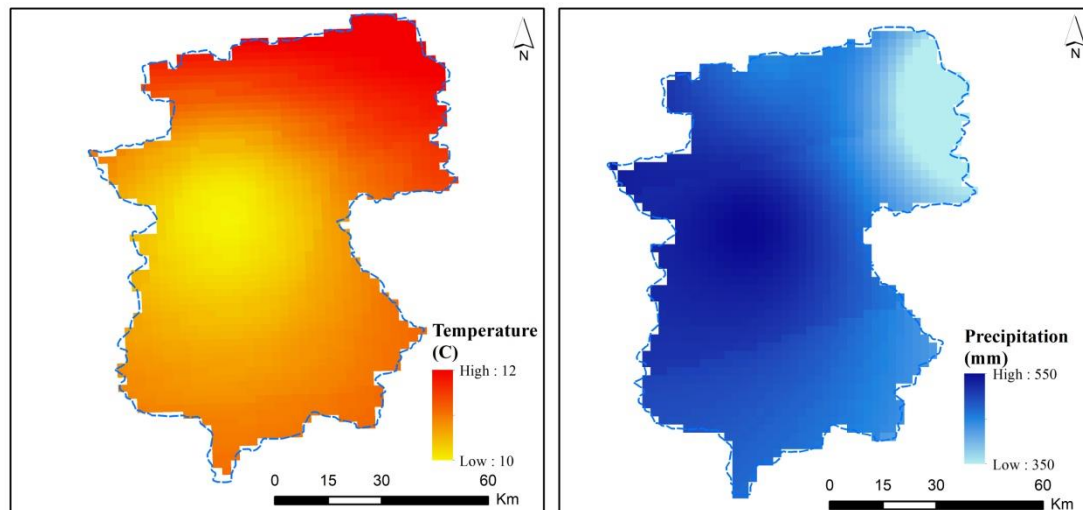


Figure 2. Temperature and precipitation maps for the western part of the Porsuk Basin



Figure 3. One of the river regulators in Porsuk Stream channel

## 2. METHODOLOGY

The study is based on the flood scenario in which the regulator covers fail to open in high flow conditions. Maximum discharges with return periods of 50 ( $Q_{50}$ ), 100 ( $Q_{100}$ ), and 200 ( $Q_{200}$ ) years were estimated by using probability distribution function.

Field and desk studies were carried out simultaneously in the study based on the flood scenario to compile the flood inundation maps. Figure 4 outlines the methodology followed in the study.

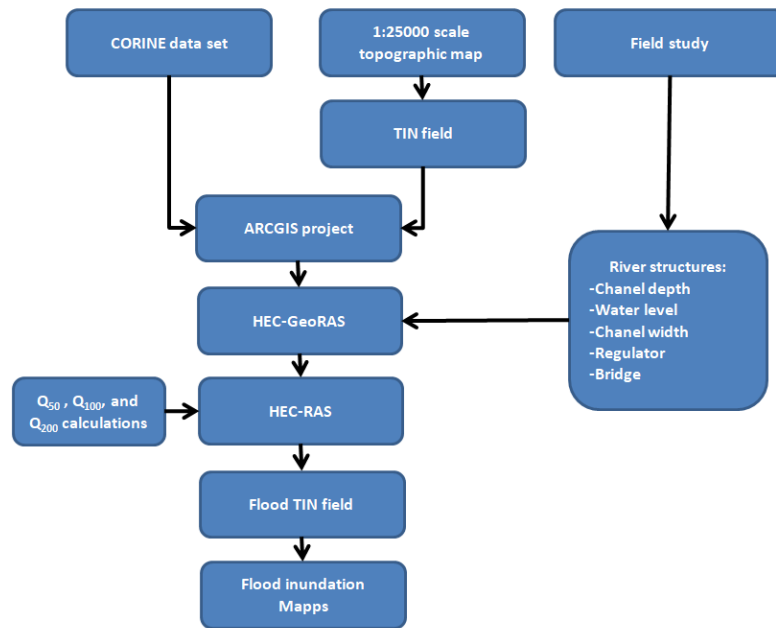


Figure 4. Study methodology

In this study, the Hydrologic Engineering Center’s River Analysis System (HEC-RAS) and Geographic Information System (GIS) software were preferred for spatial mapping. ArcGIS GIS software and its special extensions Hec-GeoRAS were used for hydraulic modeling, mapping, and analyses.

The parameters required for analyses and calculations were measured directly during the field study. In the Eskişehir city center, measurements were taken along the Porsuk Stream channel. The channel depths, water levels, and channel widths were measured for whole regulators before and after with a 100 m-long tape measure. The digital terrain model of the route taken by the Porsuk Stream channel in the Eskişehir city center was created in the GIS by using the contour lines on the 1:25000-scale topographic maps. The dimension information collected during the field studies was added to the digital terrain model. Hence, the stage at which the increase in the flow of Porsuk Stream, based on the flood scenario, would turn into flooding could be accurately detected.

$Q_{50}$ ,  $Q_{100}$ , and  $Q_{200}$  were calculated by using probability distribution function. In general, flood frequency analysis and inundation analysis studies depend on the data of the study field (flow, precipitation, temperature, etc.) and variable time parameter (Moel et al., 2009). Statistical estimation methods are commonly used in such studies, which involve highly complex and large datasets, greatly helping the interpretation and evaluation of complex datasets (Bedient and Huber, 2002).

Log-Normal (LN), Gumbel, and Log-Pearson Type III (LPT III) are commonly used probability distribution functions for maximum flow estimates in the literature (Cürebal et al., 2016; Utlu et al., 2020; Ahad et al., 2022).

The LN, distribution is a one-tailed probability distribution for any random variable whose logarithm is normally distributed (Crow and Shimizu, 1987). The hydrological variable may be skewed to the right for some reasons. In this case, the frequency does not fit the normal distribution, but since this variable is functionally normal, its logarithms fit the normal distribution (Usul, 2013).

If  $y = \log x$  has a normal distribution with probability density function is given by equation 1.

$$f(x) = \frac{1}{\sigma_y e^{y/\sqrt{2\pi}}} e^{-(y-\mu_y)^2/2\sigma_y^2}, \quad x > 0 \quad [1]$$

In the equation  $f(x)$  represents the probability density function,  $\sigma_y$  represents the standard deviation of  $y$ , and  $\mu_y$  represents the mean of  $y$  (Uslu, 2013).

Gumbel (1958) developed the Gumbel extreme values theory by considering the distribution of the smallest or largest values in repeated samples. In fact, the theory is a special probability function developed by Gumbel for floods. According to the Gumbel distribution, a flood is the largest of the 365 daily flows, and an annual series of flood flows represents a succession of principal values of flows (Ahad et al., 2022). The theory of extreme values is concerned with the distribution of the largest or smallest observations occurring in each repeated sample group (Uslu, 2013).

The probability of a flood equal to or greater than  $x$  in the Gumbel distribution is given by equation 2.

$$p = 1 - e^{-e^{-y}} \quad [2]$$

In the equation,  $p$  represents the probability of flooding, and  $y$  represents the special variable (Uslu, 2013). The value of  $y$  is determined by equation 3.

$$y = a(x - x_o) \quad [3]$$

In the equation,  $y$  represents the flood value corresponding to the probability of  $p$ .  $a$  represents the dispersion or scale parameter, and  $x_o$  represents mode value of the distribution.

When the observation period is long ( $n \geq 30$ ), the values of  $y_n$  and  $\sigma_n$  become constant. In this case,  $a$  and  $x_o$  values are calculated by using equation 4 and 5.

$$a = \frac{1.28255}{\sigma_x} \quad [4]$$

$$x_o = \bar{x} - \frac{0.778}{a} \quad [5]$$

One of the most widely used distributions in flood analyses is the LPT III distribution (Uslu, 2013; Ahad et al., 2022). The LPT III distribution is a skewed distribution bounded by the left side. Since the skewness coefficient is sensitive to extreme events, it is not suitable for small samples (Uslu, 2013). When the skewness coefficient is zero, the LPT III is identical to the log-normal distribution. Flow data ( $Q$ ) is obtained by taking the inverse logarithm of the value ( $Z_T$ ), which is obtained by using equation 6 (IACWD, 1982; Uslu, 2013).

$$Z_T = \overline{\log X} + K \sigma_{\log X} \quad [6]$$

In the equation,  $\overline{\log X}$  represents the mean value of the logarithms of the flow data for the years,  $K$  represents the flood frequency factor coefficient, and  $\sigma_{\log X}$  represents the standard deviation value of the logarithms of the flow data for the years. The standard deviation of the flow data and skewness coefficient of the flow data are obtained by using equation 7 and 8.

$$\sigma_{\log X} = \sqrt{\frac{\sum (\log x - \overline{\log x})^2}{N-1}} \quad [7]$$

$$C_s = \frac{N \sum (\log x - \overline{\log x})^2}{(N-1)(N-2)(\sigma_{\log x})^2} \quad [8]$$

In this study, for evaluating the suitability of different probability distributions, Kolmogorov–Smirnov (K-S) goodness-of-fit test is used (Yevjevich, 1972). The K-S test is used to decide whether a sample comes from an assumed continuous distribution and is based on the empirical cumulative distribution function (Kolmogorov, 1933; Smirnov, 1939, Yevjevich, 1972).

The K-S statistic value (*D*) is calculated by using equation 9.

$$D = \text{Max } |F(x) - P(x)| \quad [9]$$

In the equation, *F* (*x*) represents the goodness of fit of a theoretical distribution function, *P* (*x*) represents the empirical distribution function. If the test statistic is greater than the critical value at a chosen significance level, the hypothesis is rejected. In this study, the decision was made according to the critical value at the significance level of 0.05 ( $\alpha$ ). For significance level of 0.05 (*n*=76), the critical value is 0.1558. The K-S statistic values are given in table 3.

Table 3. K-S statistic value

<b>Probability distribution function</b>	<b>D</b>
Log-Normal	0.1696
Gumbel	0.1599
Log-Pearson Type III	0.1158

As a result of the K-S test, it was decided that the most suitable distribution for the data set was LPT III. The LPT III distribution is a statistical method based on annual maximum flow data and used in the estimation of maximum discharges at varying intervals in rivers (Rao and Hamed, 2000; Özdemir, 2008).

Flow data used throughout the study were obtained from the General Directorate of Electrical Power Resources Survey and Development Administration (in Turkish, Elektrik İşleri Etüd İdaresi, “EİE”). Gauging station E1203 is 855 m above sea level and has a drainage area of ~39000 km<sup>2</sup>. Gauging station E1203 is situated 40 km southwest of the Eskişehir city center. The existence of long-term and continuous observation data and the station’s location behind the dam weir were the main reasons for selecting that station. The time series including data on monthly discharge for 1936-2011 from the corresponding station were used.

By taking the CORINE data for 2012 as reference, the land use distribution of the Eskişehir city center was determined. Thus, the degree to which the settlement areas, industrial areas, agricultural areas, and airport would be affected by the floods was revealed.

Topographic data were prepared by using ArcGIS and then transferred to the HEC-GeoRAS module. The cross-sections along the 16.9 km line were formed in the module (Figure 5). Water levels and flooded areas were determined with the HEC-RAS program according to the *Q*<sub>50</sub>, *Q*<sub>100</sub>, and *Q*<sub>200</sub> calculated with LPT III.

In the study area, Porsuk Stream moves in a concrete open channel. Therefore, Manning’s Roughness Coefficient was taken as 0.012 for the calculations.

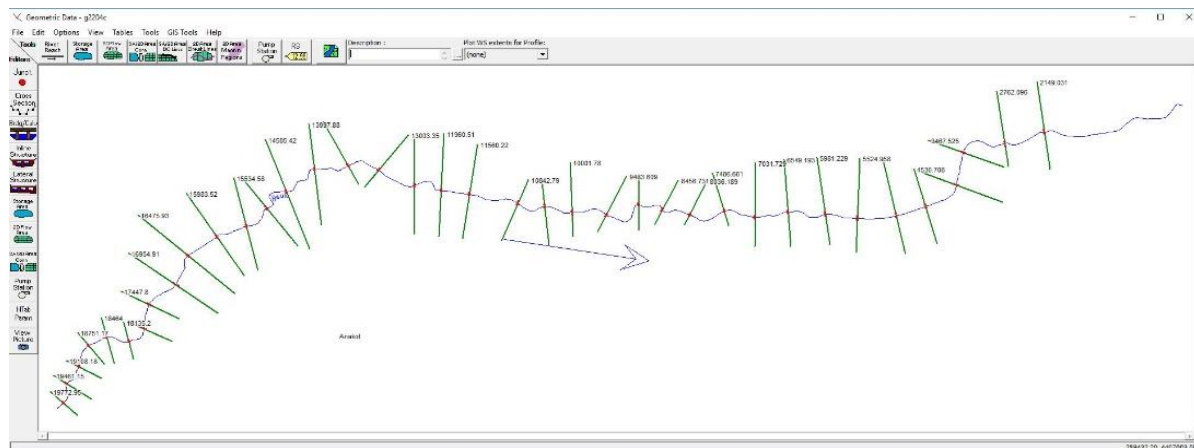


Figure 5. Cross-sections created for the flow of Porsuk Stream in Eskişehir

### 3. RESULTS AND DISCUSSION

Expected maximum floods at E1203 gauging station for  $Q_{50}$ ,  $Q_{100}$ , and  $Q_{200}$  were calculated by using annual maximum discharges. Probable maximum discharges were determined using the LPT III method and are shown in Table 4. As a result of the LPT III calculations, estimated maximum discharges with return periods of 50, 100, and 200 years are  $136.54 \text{ m}^3/\text{s}$ ,  $164.30 \text{ m}^3/\text{s}$ , and  $194.46 \text{ m}^3/\text{s}$ , respectively (Figure 6).

Table 4. Maximum discharges for  $Q_{50}$ ,  $Q_{100}$ , and  $Q_{200}$

Return period (T)	$K_{\text{lower}}$	$K_{\text{upper}}$	Slope	$K_{\text{calculated}}$	$\text{Log}Q_{\text{Tr\_cfs}} (Z_T)$	$Q_{\text{Tr\_cfs}} (Q)$
50	1.94	2.0	0.55	1.98	2.13	136.54
100	2.17	2.252	0.74	2.23	2.21	164.30
200	2.38	2.482	0.94	2.46	2.28	194.46

The Porsuk Stream passing through the Eskişehir city center was turned into a fixed channel that is about thirty meters wide and six meters deep. The flow in the channel was modeled with HEC-RAS software according to the maximum discharges with return periods of 50, 100, and 200 years. In the case of open regulators,  $Q_{50}$  and  $Q_{100}$  do not cause any flooding. On the contrary,  $Q_{200}$  would cause a very small flood, but the flood would not result in an important inundation.

For the case in which the regulators could not open for any reason, and the expected maximum discharges would have to flow over a two-meter-deep water load, different flood areas emerge.

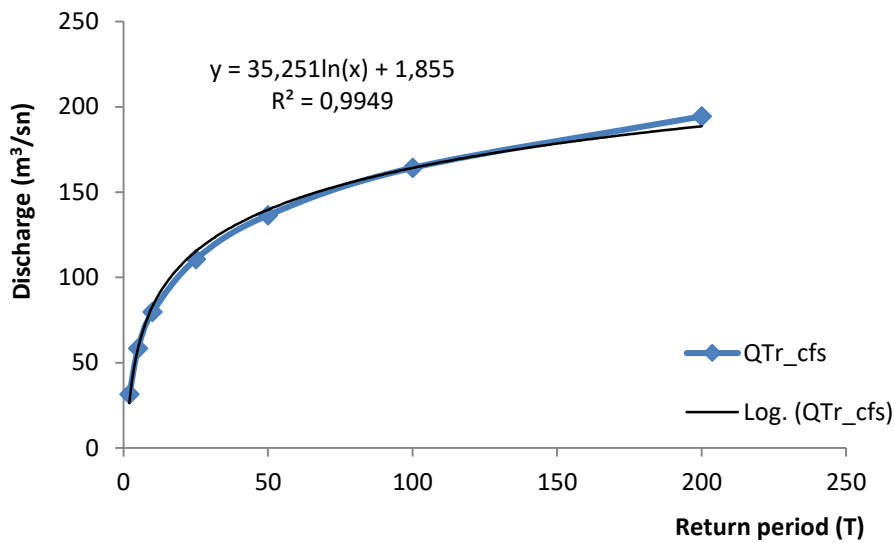


Figure 6. Flood frequency of study area

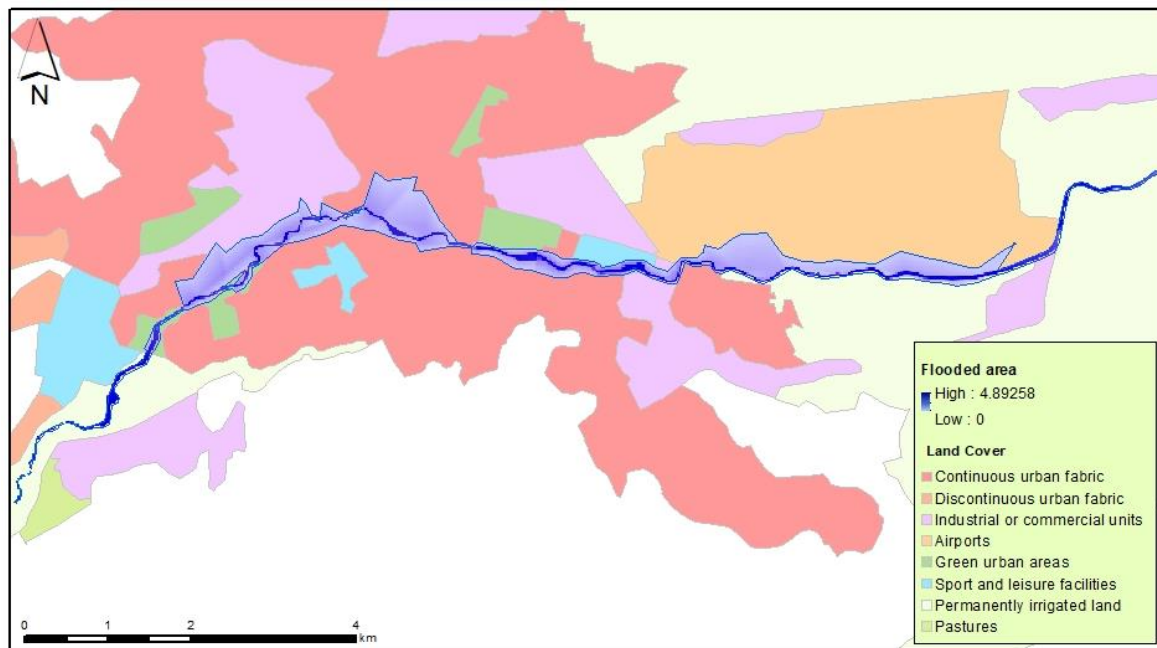
The maximum discharge with the return periods of 50 years ( $Q_{50}$ ) is 136.54 m<sup>3</sup>/s, and it is estimated that a total area of 33.20 km<sup>2</sup> would be flooded in the city center in the case of its occurrence. Table 5 shows the areas in the city center that would be covered with flood water with respect to land use type. This reveals that 1.27 km<sup>2</sup> of the settlement areas would be flooded and that  $Q_{50}$  would cause the inundation of 0.42 km<sup>2</sup> of agricultural areas. Of the total flood area, 40% would be settlement areas, 25% would be the airport, 13% would be agricultural lands, 11% would be green areas, 8% would be industrial areas, and 3% would be sport facilities.

Table 5. Flooded areas in the city center for  $Q_{50}$

Land Cover	Area (km <sup>2</sup> )	Percentage (%)
Continuous urban fabric	1.27	40
Industrial or commercial units	0.26	8
Airport	0.79	25
Sport and leisure facilities	0.11	3
Green urban areas	0.34	11
Permanently irrigated land	0.42	13
<b>Total</b>	<b>3.20</b>	<b>100</b>

Figure 7 shows the flood inundation map created by using the data obtained in the study. The figure reveals that the flood waters mostly threaten settlement areas in the case of  $Q_{50}$ .

The maximum discharge with the return periods of 100 year ( $Q_{100}$ ) is 164.30 m<sup>3</sup>/s, and it is estimated that a total area of 4.03 km<sup>2</sup> would be flooded in the city center in the case of its occurrence. Table 6 shows the areas in the city center that would be covered with flood water with respect to land use type. This reveals that 1.46 km<sup>2</sup> of the settlement areas would be flooded and that  $Q_{100}$  would cause the inundation of 0.49 km<sup>2</sup> of agricultural lands. Of the total flood area, 36% would be settlement areas, 31% would be the airport, 12% would be agricultural lands, 10% would be green areas, 8% would be industrial areas, and 3% would be sport facilities.

Figure 7. Flood inundation map for  $Q_{50}$ Table 6. Flooded areas in the city center for  $Q_{100}$ 

Land Cover	Area (km <sup>2</sup> )	Percentage (%)
Continuous urban fabric	1.46	36
Industrial or commercial units	0.33	8
Airport	1.24	31
Sport and leisure facilities	0.12	3
Green urban areas	0.39	10
Permanently irrigated land	0.49	12
<b>Total</b>	<b>4.03</b>	<b>100</b>

Figure 8 shows the flood inundation map created by using the data obtained in the study. The figure reveals that the flood waters would especially threaten the settlement areas and the airport in the case of  $Q_{100}$ .

The maximum discharge with the return periods of 200 year ( $Q_{200}$ ) is 194.46 m<sup>3</sup>/s, and it is estimated that a total area of 4.48 km<sup>2</sup> would be flooded in the city center in the case of its occurrence. Table 7 shows the areas in the city center that would be covered with the flood water with respect to land use type. This reveals that 1.58 km<sup>2</sup> of the settlement areas would be flooded and that  $Q_{200}$  would cause the inundation of 0.55 km<sup>2</sup> of agricultural lands. Of the total flood area, 35% would be settlement areas, 33% would be the airport, 12% would be agricultural lands, 9% would be green areas, 7% would be industrial areas, and 3% would be sport facilities.

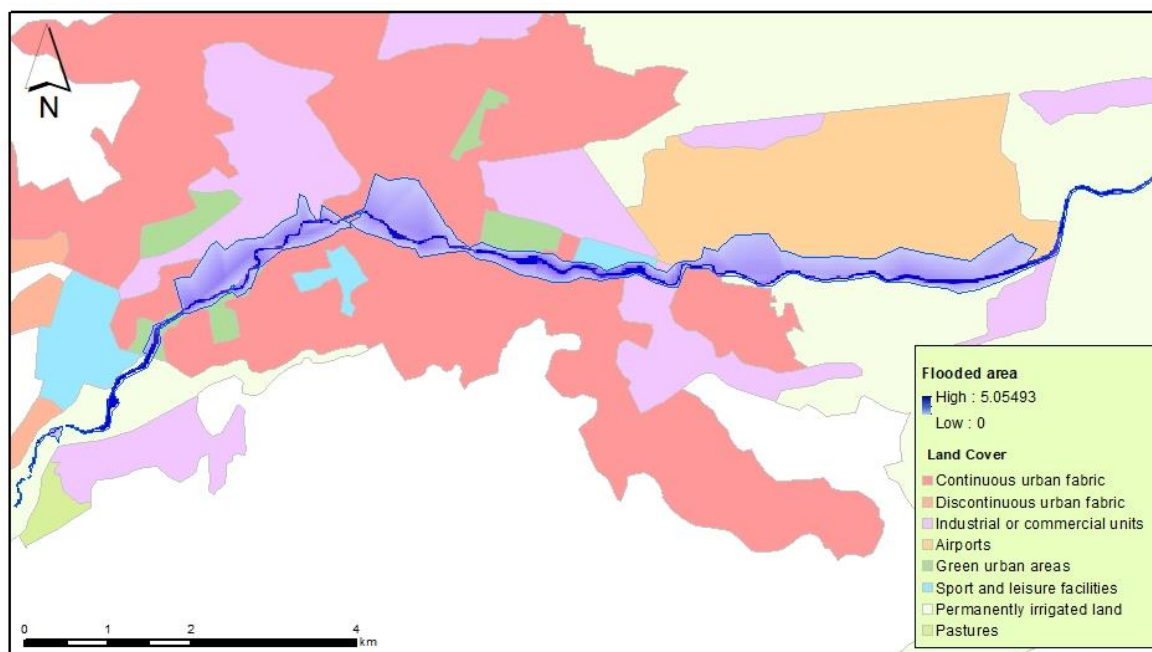


Figure 8. Flood inundation map for Q<sub>100</sub>

Table 7. Flooded areas in the city center for Q<sub>200</sub>

Land Cover	Area (km <sup>2</sup> )	Percentage (%)
Continuous urban fabric	1.58	35
Industrial or commercial units	0.30	7
Airport	1.50	33
Sport and leisure facilities	0.13	3
Green urban areas	0.42	9
Permanently irrigated land	0.55	12
<b>Total</b>	<b>4.48</b>	<b>100</b>

Figure 9 shows the flood inundation map created by using the data obtained in the study. Similar to the case of Q<sub>100</sub>, the flood waters would threaten settlement areas and the airport almost at equal levels.

The results of the study show that, in the case of the movement of the flood discharge in a two-meter-deep channel, floods would occur in the city center with different distributions under different flow conditions.

The time series of Gauging station E1203 for the years 1970-2011 which is located upstream of the Porsuk Dam were used in the study. Furthermore, Sarısu, Sabuncupınarı, and Ilıca streams are joined to the Porsuk Stream from downstream of Gauging station E1203. The discharge values of those tributaries are not included in the study because of the location of the Gauging station E1203. Within this scope, considering the water amount carried by the side tributaries, the Q<sub>50</sub>, Q<sub>100</sub>, and Q<sub>200</sub> discharges would be expected to be higher than the calculated values.

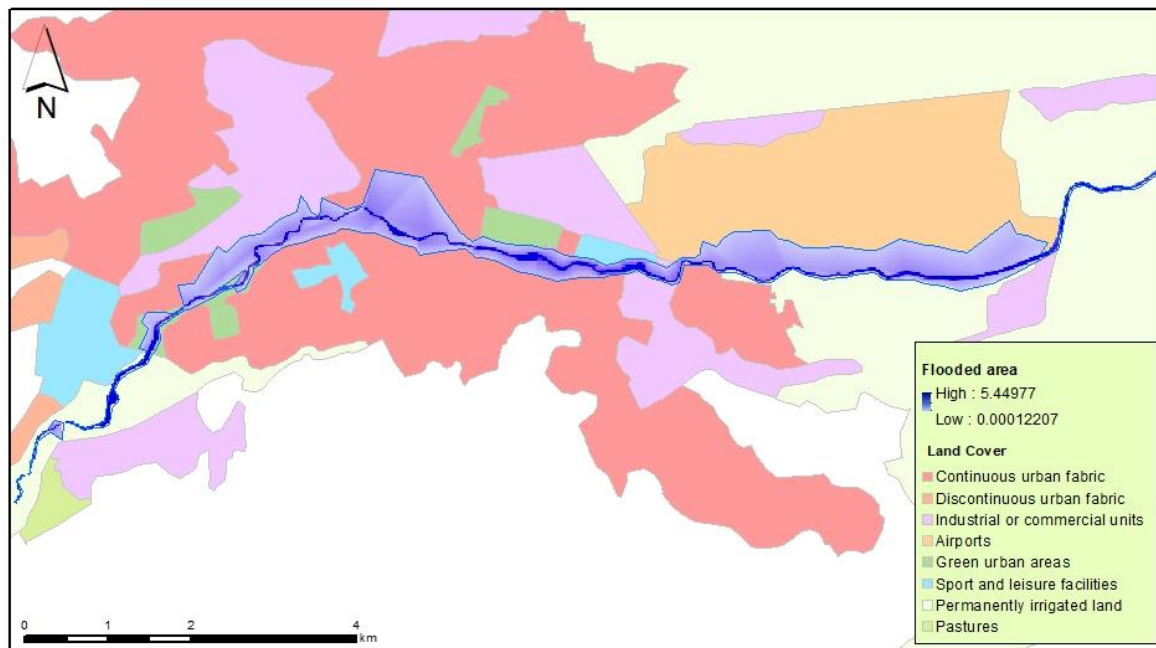


Figure 9. Flood inundation map for  $Q_{200}$

There are numerous studies in the literature for Porsuk Stream in which used different scenarios and flood discharges are calculated by using the LPT III distribution. Bayazit et al. (2019), aimed to develop the flood risk analysis of Porsuk Stream at recurring periods of 50, 100, and 1000 years. Their turning periods of 50, 100, and 200 years discharge of Porsuk Stream which is calculated as  $51.83 \text{ m}^3/\text{s}$ ,  $60.15 \text{ m}^3/\text{s}$ , and  $68.92 \text{ m}^3/\text{s}$  respectively. Those calculated values are smaller than the present study. In our opinion, that may be due to time series belonging to a different gauging station located downstream of the dam have been used. In addition, due to the  $Q_{50}$ ,  $Q_{100}$  flood discharges, their flood inundation maps have differences from the present study. Moreover, it is thought that the main reason for this is that they do not consider the artificial bed geometry and flow characteristics that Porsuk Stream in the city center. Using the MIKE 11 method, Karaer et al. (2018) created a flood model for Porsuk Stream. In their study, they calculated the  $Q_{50}$ ,  $Q_{100}$ , and  $Q_{200}$  flood discharges as  $1083 \text{ m}^3/\text{s}$ ,  $1100 \text{ m}^3/\text{s}$ , and  $1108 \text{ m}^3/\text{s}$ , respectively using the LPTT III distribution. The values calculated by those researchers are considerably higher than those found in this study. Gauging station was not clearly stated in their research. Hence, the main reason why the LPTIII distribution results are quite different is thought to be due to the use of time series belonging to a different gauging station than the one used in this study. The location of the measurement stations, the methodology used, and the input data used in these studies can also lead to different results. Haltas and others (2016) investigated the distribution of a flood wave occurring in the Eskişehir city center on the basis of a destruction scenario that could occur at Porsuk Dam. Their results showed that the channel could not resist the flood discharge and that an area of  $127 \text{ km}^2$  would be affected by the flood. The flood discharge value they found for the worst-case scenario is close to the  $Q_{200}$  flood discharge found in this study.

#### 4. CONCLUSION

The abundance of impervious surfaces in urban areas increases the risk of flooding. Most of the precipitation starts to run off on impervious surfaces. The increase in impervious areas in cities and the fact that a larger proportion of rainfall turns into runoff also increases the risk of flooding.

In addition to this, keeping the water level too high in the river channel running through the city can make the city much more vulnerable in case of flooding.

In the study, a special flood scenario was created for Porsuk Stream, which passes through the Eskişehir city center. The scenario is based on the failure of the regulator covers to open and the movement of a sudden flow two meters deep over the existing water body in the channel. According to the scenario, flood inundation maps were created for the  $Q_{50}$ ,  $Q_{100}$ , and  $Q_{200}$  discharges were calculated by using the LPT III distribution.

The results of the study indicated that floods would occur in the city center for various maximum flows as  $Q_{50}$ ,  $Q_{100}$ , and  $Q_{200}$  discharges. The areas in the city center that would be flooded by the  $Q_{50}$ ,  $Q_{100}$ , and  $Q_{200}$  discharges are 3.20 km<sup>2</sup>, 4.03 km<sup>2</sup>, and 4.48 km<sup>2</sup>, respectively. The areas with the highest risk are the settlement areas and the airport. Green areas, industrial areas and sports facilities are also vulnerable to flooding.

To ensure the rapid discharge of the Porsuk channel through the regulators, the maintenance of the regulator covers should not be neglected, and the covers should be tested regularly. It is expected that the regulator-based flood outputs of this study will help the decision-makers to reach more accurate results. It is also necessary to take precautions against the possibility of a long-term power outage. In such a case, it is necessary to install devices that will enable the regulators to operate independently of the city's electricity network.

## REFERENCES

- Ahad, U., Ali, U., Inayatullah, M., Rauf Shah, A., (2022). Flood Frequency Analysis: A Case Study of Pohru River Catchment, Kashmir Himalayas, India. *Journal of the Geological Society of India*, 98(12), 1754-1760
- Alfieri L., Salamon P., Bianchi A., Neal J., Bates P., Feyen L., (2014) Advances in pan-European flood hazard mapping. *Hydrol Process* 28(13):4067–4077. <https://doi.org/10.1002/hyp.9947>
- Amellah O., El Morabiti K., Ouchar Al-djazouli M., (2020) Spatialization and assessment of flood hazard using 1D numerical simulation in the plain of Oued Laou (North Morocco). *Arab J Geosci* (13) 635. <https://doi.org/10.1007/s12517-020-05592-4>
- Ashley R.M., Balmforth D.J., Saul A.J., Blanskby J.D., (2005) Flooding in the future - predicting climate change. risks and responses in urban areas. *Water Sci Technol.* 52(5): 265-273. <https://doi.org/10.2166/wst.2005.0142>
- Baker V.R., (2013) Global late Quaternary fluvial paleohydrology with special emphasis on paleofloods and megafloods, in: *Fluvial Geomorphology*, edited by: Wohl, EE, Vol. 9, Treatise on Geomorphology, Academic Press, San Diego, 511–527
- Bayazit Y., Bakiş R., Koç C., Kaya T., Özdemir N., (2019) Formation of Eskişehir Province Flood Maps with Using of Geographical Information Systems. *Journal of Geoscience and Environment Protection*. 7(11). 151. <https://doi.org/10.4236/gep.2019.711011>
- Bedient P.B., Huber W.C., (2002) *Hydrology and Floodplain Analysis*. Prentice Hall. USA.
- Berghuijs W.R., Allen S.T., Harrigan S., Kirchner J.W., (2019) Growing spatial scales of synchronous river flooding in Europe. *Geophysical Research Letters*, 46(3), 1423-1428. <https://doi.org/10.1029/2018GL081883>
- Berz G., (2001) Flood disasters: lessons from the past-worries for the future. *Proceedings of The Institution of Civil Engineers-Water Maritime and Energy*. 148(1). 57-58. <https://doi.org/10.1680/wame.2000.142.1.3>

- Bharath R., Elshorbagy A., (2018) Flood mapping under uncertainty: a case study in the Canadian prair. *Natural Hazards* 94: 537. <https://doi.org/10.1007/s11069-018-3401-1>
- Chang H., Franczyk J., (2008) Climate Change, Land Use Change, and Floods: Toward an Integrated Assessment. *Geography Compass*. 2(5). 1549-1579. <https://doi.org/10.1111/j.1749-8198.2008.00136.x>
- Chen J., Hill A.A., Urbano L.D., (2009) A GIS-based model for urban flood inundation. *J Hydrol* 373(1):184–192. <https://doi.org/10.1016/j.jhydrol.2009.04.021>
- Costabile, P., Costanzo, C., Ferraro, D., Macchione, F., Petaccia, G., (2020) Performances of the new HEC-RAS version 5 for 2-D hydrodynamic-based rainfall-runoff simulations at basin scale: Comparison with a state-of-the art model. *Water*, 12(9), 2326.
- CRED (2003) International Disaster Database. Centre for Research on the Epidemiology of Disasters. Brussels. Belgium.
- Crow, E.L., Shimizu, K., (1987) Lognormal distributions. New York: Marcel Dekker.
- Cutter S.L., Emrich C.T., Gall M., Reeves R. (2018) Flash flood risk and the paradox of urban development. *Natural Hazards Review*, 19(1), 05017005. [https://doi.org/10.1061/\(asce\)nh.1527-6996.0000268](https://doi.org/10.1061/(asce)nh.1527-6996.0000268)
- Cürebali I., Efe R., Özdemir H., Soykan A., Sönmez S., (2016) GIS-based approach for flood analysis: case study of Keçidere flash flood event (Turkey). *Geocarto International*, 31(4), 355-366. <https://doi.org/10.1080/10106049.2015.1047411>
- Çiçek İ., Duman N., (2015) Seasonal and annual precipitation trends in Turkey. *Carpathian Journal of Earth and Environmental Sciences*, 10(2), 77-84.
- Dahri N., Abida H., (2020) Causes and impacts of flash floods: case of Gabes City, Southern Tunisia. *Arab J Geosci* (13) 176. <https://doi.org/10.1007/s12517-020-5149-7>
- Dottori F., Szewczyk W., Ciscar J.C., Zhao F., Alfieri L., Hirabayashi Y., Bianchi A., Mongelli I., Frieler K., Betts R.A., Feyen L. (2018) Increased human and economic losses from river flooding with anthropogenic warming. *Nature Climate Change*, 8(9), 781-786.
- Dutta D., Herath S., (2004) Trend of floods in asia and proposal for flood risk management with integrated river basin approach. In *Proceeding of the Second International Conference of Asia-Pacific Hydrology and Water Resources Association*. Singapore. Volume I; 128-137.
- Erkal T., Taş B., (2013) Jeomorfoloji ve İnsan. Yeditepe: İstanbul
- Gumbel, E.J. (1958). *Statistics of extremes*. Columbia University Press: New York.
- Haltas I., Elçi S., Tayfur G., (2016) Numerical simulation of flood wave propagation in two-dimensions in densely populated urban areas due to dam break. *Water Resources Management*. 30(15). 5699-5721.
- Hirabayashi Y., Mahendran R., Koirala S., Konoshima L., Yamazaki D., Watanabe S., Kim H., Kanae S., (2013) Global flood risk under climate change. *Nature Climate Change*. 3(9). p.816.
- Huong H.T.L., Pathirana A., (2013) Urbanization and climate change impacts on future urban flooding in Can Tho city. Vietnam. *Hydrol Earth Syst Sc.* 17(1): 379-394. <https://doi.org/10.5194/hess-17-379-2013>
- IACWD (Interagency Advisory Committee on Water Data). (1982) Guidelines for Determining Flood Frequency. Bulletin#17B of Hydrology Subcommittee. Office of Water Data Coordination. US Geological Survey. Reston. V.A.

Kaya Melisa C., Varol N., Gungor O., (2020) Investigation of the role of land use method on increased flood vulnerability in rural areas: a case study on Güneysu River, Turkey. Arab J Geosci (13) 578. <https://doi.org/10.1007/s12517-020-05627-w>

Karaer F., Koparal A., Tombul M., (2018) Environmental risk determination of flood in Porsuk River basin via one-dimensional modelling. Appl. Ecol. Environ. Res. 16. 4969-4983. [https://dx.doi.org/10.15666/aeer/1604\\_49694983](https://dx.doi.org/10.15666/aeer/1604_49694983)

Kleinen T., Petschel-Held G., (2007) Integrated assessment of changes in flooding probabilities due to climate change. Climatic Change. 81(3). 283-312.

Kolmogorov A.N., (1933) Sulla determinazione empirica di una legge di distribuzione. G. Ist. Attuari,4(1), 83-91.

Korkmaz, M., (2022a) Drought Research and Trend Analysis in Yozgat Province (Turkiye). Engineering Sciences, 17(3), 21-34.

Korkmaz, M., (2022b) Nehirlerde Taşkın Tekerrür Debisi Hesabı ve Taşkın Risk Değerlendirmesi. El-Cezeri, 9(2), 532-541.

Koylu Z., (2008) XX. Yüzyılın Başlarında Eskişehir / Eskişehir at the Beginning of the 20th Century. Atatürk Araştırma Merkezi Dergisi Cilt: XXIV. Sayı: 71

Li G.F., Xiang X.Y., Tong Y.Y., Wang H.M., (2013) Impact assessment of urbanization on flood risk in the Yangtze River Delta. Stoch Env Res Risk A. 27(7): 1683-1693.

Masood M., Takeuchi K., (2012) Assessment of flood hazard, vulnerability and risk of mid-eastern Dhaka using DEM and 1D hydrodynamic model. Nat Hazards 61(2):757-770.

McCabe G.J.J., Wolock D.M., (1997) Climate change and the detection of trends in annual runoff. Clim.Res.8.129-134

Milly P.C.D., Wetherald R.T., Dunne K.A., Delworth T.L., (2002) Increasing risk of great floods in a changing climate. Nature. 415(6871). 514.

Moel H., Alphen J.V., Aerts J.C.J.H., (2009) Flood maps in Europe— methods, availability and use. Nat. Hazards Earth Syst. Sci. 9. 289-301

Namara, W. G., Damisse, T. A., Tufa, F. G., (2022) Application of HEC-RAS and HEC-GeoRAS model for Flood Inundation Mapping, the case of Awash Bello Flood Plain, Upper Awash River Basin, Oromiya Regional State, Ethiopia. Modeling Earth Systems and Environment, 8(2), 1449-1460.

OSİB (Orman ve Su İşleri Bakanlığı). (2015). Ulusal Taşkın Yönetimi Strateji Belgesi ve Eylem Planı. Ankara.

Özdemir H., (2008) Havran Çayı'nın (Balıkesir) Taşkın Sıklık Analizinde Gumbel ve Log Pearson Tip III Dağılımlarının Karşılaştırılması. Coğrafi Bilimler Dergisi. 6(1). 41-53.

Özdemir A., Leloğlu U.M., (2014) Climate change impact assessment on river basin: Sarisu-Eylıklar River, Turkey. In 2nd International sustainable watershed management conference. SuWaMa (pp. 103-112).

Pinos J., Quesada-Román A., (2021) Flood risk-related research trends in latin america and the caribbean. Water, 14(1), 10. <https://doi.org/10.3390/w14010010>

Quiroga, V. M., Kurea, S., Udoa, K., Manoa, A., (2016) Application of 2D numerical simulation for the analysis of the February 2014 Bolivian Amazonia flood: Application of the new HEC-RAS version 5. Ribagua, 3(1), 25-33.

Rao A.R., Hamed K.H., (2000) Flood Frequency Analysis. CRS Press. USA.

Sarış F., Hannah D.M., Eastwood W.J., (2010) Spatial variability of precipitation regimes over Turkey. Hydrological Sciences Journal. 55. 234-249. <https://doi.org/10.1080/02626660903546142>

Scalenghe R., Marsan F., (2009) The anthropogenic sealing of soils in urban areas. Landscape and Urban Planning, 90(1-2),1-10. <https://doi.org/10.1016/j.landurbplan.2008.10.011>

Shi J., Cui L., Tian Z., (2020) Spatial and temporal distribution and trend in flood and drought disasters in East China. Environmental Research, 185, 109406. <https://doi.org/10.1016/j.envres.2020.109406>

Simonovic S.P., (2012) Floods in a changing climate: risk management. Cambridge University Press. United Kingdom

Strohbach, M. W., Döring, A. O., Möck, M., Sedrez, M., Mumm, O., Schneider, A. K., Schröder, B., (2019). The "hidden urbanization": Trends of impervious surface in low-density housing developments and resulting impacts on the water balance. Frontiers in Environmental Science, 7, 29. <https://doi.org/10.3389/fenvs.2019.00029>

Şimşek G., (2014) River Rehabilitation with Cities in Mind: The Eskişehir Case. METU Journal of the Faculty of Architecture. 31(1). <http://dx.doi.org/10.4305/metu.jfa.2014.1.2>

Tate, E., Maidment, D., (1999) Floodplain mapping using HEC-RAS and ArcView GIS. University of Texas at Austin Center For Research in Water Resources.

TBMM (1950) Eskişehir sel baskınından zarar görenler için yaptırılacak meskenler hakkında kanun tasarısı (1/765). Meclis Tutanağı S. Sayısı:283. Ankara

Usul, N. (2013). Mühendislik Hidrolojisi. ODTU Yayıncılık: Ankara.

URL 1, Economic Losses. Poverty and Disasters: 1998-2017; [https://www.cred.be/downloadFile.php?file=sites/default/files/CRED\\_Economic\\_Losses\\_10oct.pdf](https://www.cred.be/downloadFile.php?file=sites/default/files/CRED_Economic_Losses_10oct.pdf). [Date of access : Nov 01 2019].

URL 2, EM-DAT (Emergency Events Database) OFDA/CRED International Disaster Database. Universite Catholique de Louvain. Brussels. [www.cred.be/emdat](http://www.cred.be/emdat). [Date of access : Nov 08 2019].

URL 3, <https://tabb-dokuman.afad.gov.tr/>. [Date of access : Nov 11 2019].

Utlı M., Şimşek M., Öztürk M.Z., (2020) 1d Taşkın modelleri açısından topo SYM ve ALOS SAM verilerinin karşılaştırılması: Alara Çayı örneği (Antalya). Aegean Geographical Journal, 29(2), 161-177.

Ward R.C., (1978) Floods - a geographical perspective. Published by: Macmillan.

Yang, J., Townsend, R. D., Daneshfar, B., (2006) Applying the HEC-RAS model and GIS techniques in river network floodplain delineation. Canadian Journal of Civil Engineering, 33(1), 19-28.

Yevjevich V., (1972) Probability and Statistics in Hydrology. Water Resources Publications, Fort Collins, Colorado.